Comparative study of the magnetic form factors of transition-metal ions

D. C. Khan, S. M. Kirtane, and J. K. Sharma
Department of Physics, Indian Institute of Technology, Kanpur, U.P. 208016, India
(Received 8 June 1978; revised manuscript received 12 May 1980)

The present paper reports the results of reformulation of Trammell's method in terms of an elaborate computer program for calculation of the magnetic form factor for spin as well as orbital moment interaction with neutrons for any given cation wave function in a crystal. This provides an opportunity for making a comparative study of the form factors and hence magnetization density distribution of transition-metal ions in various crystal environments. Spherical and aspherical parts of the form factors of transition-metal difluorides are calculated. The spherical form factor shows an expansion of 10%, a contraction of 3%, and an expansion of 15%, with respect to the free-ion spin-only curve of CoF_2, FeF_2, and NiF_2, respectively. A comparative study of the form factors of X^{2+} ions ($X^{2+} = Fe^{2+}$, Co^{2+}, Ni^{2+}) in XF_2, KXF_3, and XO compounds is undertaken. It is found that the crystalline environment, through the quenched orbital effect, tends to contract the magnetization density distribution with respect to the free-ion spin-only distribution. Finally, quenching is quantitatively studied by calculating the ratio of the orbital to the total magnetic moment of the ion and comparing it with experimental data.

I. INTRODUCTION

The determination of magnetization density distribution due to a transition-metal ion in a solid through a study of the magnetic form factor is a well known method in elastic neutron scattering. Form factors are calculated considering spin and orbital moments with wave functions of different degrees of sophistication, e.g., crystal-field or covalent wave functions, until the agreement with experiment is reached. In the present work Trammell's method has been reformulated in terms of an elaborate computer program for calculation of the magnetic form factor for any given cation wave function in a crystal. The form factors of cations in NiF_2, CoF_2, and FeF_2, each of which has a rutile structure, have been calculated. A complementary study has also been made where the cation is the same, e.g., Co^{2+}, but is studied in various crystal environments as in CoO, $KCoF_3$, and CoF_2. When compared with the experimental data of magnetic neutron scattering, these will provide substantial insight into the nature of magnetization distribution in a crystal and hence its magnetic state.

II. THE COMPUTATIONAL METHOD

The basic equation for the differential elastic scattering cross section in Trammell formalism[1] is well known:

$$\frac{d\sigma}{d\Omega}=\left(\frac{\gamma e^2}{mc^2}\right)^2\left|\sum_n e^{i\vec{K}\cdot\vec{n}}\langle q|\vec{H}|q\rangle\right|^2, \qquad (1)$$

where $|q\rangle$ is the crystal ground-state wave function, $\vec{n}$ the lattice vector, and $\vec{H}$ the interaction operator given by

$$\vec{H}=\sum_j e^{i\vec{K}\cdot\vec{r}_j}\vec{S}_j+\tfrac{1}{4}[\vec{l}_j f(\vec{K}\cdot\vec{r}_j)+f(\vec{K}\cdot\vec{r}_j)\vec{l}_j], \qquad (2)$$

where j runs over all the unpaired electrons of a magnetic ion. $\vec{K}$ is the neutron scattering vector.

If we assume that $|q\rangle$ can be written as a product of the state vectors of individual ions, Eq. (1) can be written as

$$\frac{d\sigma}{d\Omega}=\left(\frac{\gamma e^2}{mc^2}\right)^2\sin^2\omega\,|\vec{Q}|^2_{\vec{K}=\vec{G}},$$

where

$$\vec{Q}_{\vec{K}=\vec{G}}=[\langle q_1|\vec{H}|q_1\rangle+\langle q_2|\vec{H}|q_2\rangle e^{2\pi i(ha_2+kb_2+lc_2)}+\cdots+\langle q_u|\vec{H}|q_u\rangle e^{2\pi i(ha_u+kb_u+lc_u)}]. \qquad (3)$$

Here a_u, b_u, c_u, and $|q_u\rangle$ give the position and the wave function of the representative ion of the sublattice in the crystal, h,k,l, are the indices of a particular peak, and ω is the angle between $\vec{K}$ and $\vec{Q}$ at $\vec{K}=\vec{G}$. In the uniaxial spin structure, $\langle q|\vec{H}|q\rangle$ factors out and $\langle q|\vec{H}|q\rangle/\langle q|\vec{H}|q\rangle|_{\vec{K}=0}$ defines the form factors.

Trammell[1] assumed a form of the wave function $|q\rangle$ suitable for the rare earths and carried the analysis to a stage where the cross sections could be written in terms of $\langle g_i\rangle$ and $\langle J_i\rangle$ (integrals F^s and F^l's in his language). Blume[2] took the crystal-field state $^3\Gamma_2$ of Ni^{2+} modified by the spin-orbit coupling as the ground-state wave function for Ni^{2+} and again expanded his cross section in terms of the same integrals. Since we required the computation done for an arbitrary wave function, we did not proceed with the analytical wave function any further than Eq. (3). We broke down the wave function in one-electron spin orbitals right at this stage and used program number 1 to obtain the nonvanishing matrix elements in $\langle\psi|\vec{H}|\psi\rangle$ as well as their coefficients:

 © 1981 The American Physical Society

$$f^{\mu} = \sum_{\alpha\beta} C^{\mu}_{\alpha\beta} \langle \alpha | e^{i\vec{K}\cdot\vec{r}} | \beta \rangle + \sum_{\gamma\delta} C^{\mu}_{\gamma\delta} \langle \gamma | f(\vec{K}\cdot\vec{r}) | \delta \rangle \quad (\mu = x, y, z), \tag{4}$$

where $\alpha, \beta, \gamma, \delta$ could be any of the one-electron (or one-hole) orbitals that will exist after the application of the spin and orbital angular momentum selection rules by the program. The expression for any one cation will differ from that of another by the combination of $\alpha\beta\gamma\delta$'s and, of course, the values of the corresponding coefficients $C_{\alpha\beta}$'s and $C_{\gamma\delta}$'s. Program no. 2 expands the spin matrices $\langle \alpha | e^{i\vec{K}\cdot\vec{r}} | \beta \rangle$ and the orbital ones $\langle \gamma | f(\vec{K}\cdot\vec{r}) | \delta \rangle$ in terms of spherical harmonics Y_{lm}, Condon-Shortley coefficients[3] $C^{L}(l,m;l',m')$, and Watson-Freeman[4] integrals $\langle h_L \rangle = \int_0^{\alpha} R^2(r) h_L(Kr) r^2 dr$ and ultimately gives the values of the form factor for different peaks (h,k,l). It may be seen that the expression for f^x and f^y will contain only cross-term matrix elements, i.e., $\alpha \neq \beta$ and $\gamma \neq \delta$. Thus the Y_{lm}'s in their expansion will not contain any Y_{lo} term. Hence f^x and f^y will be completely nonspherical. On the other hand, f^z will contain both diagonal and nondiagonal terms and hence it will have both spherical and nonspherical parts.

As a check, we calculate the form factor of Ni^{2+} in NiO and compare it with the results of Blume.[2] We use the same wave function as Blume except that we work out the effect of the spin-orbit coupling in detail before proceeding for the form-factor calculation and remove the triple degeneracy of the ground state by incorporating the exchange field. Figure 1 shows that the agreement is excellent at low values of $\sin\theta/\lambda$ and at higher angles our results come closer to the experimental data.

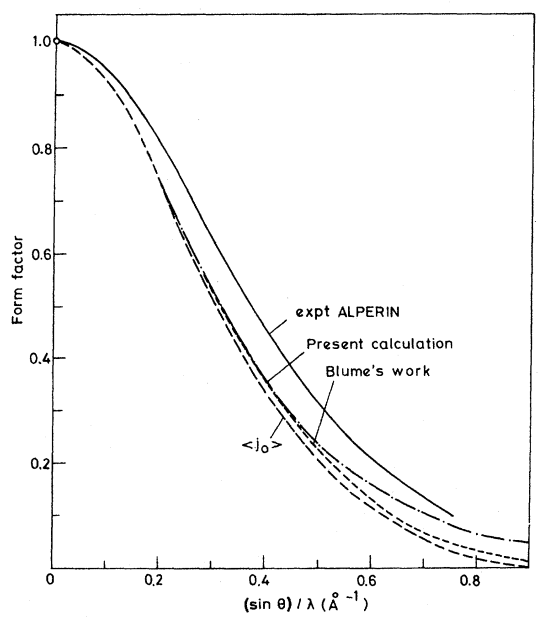

FIG. 1. Comparison of the form factors of Ni^{2+} in NiO as calculated in the present work and in the work of Blume.

III. TRANSITION-METAL DIFLUORIDES

The bulk of the present work is the use of the above program in a detailed study of the spherical and aspherical form factors of the transition-metal difluorides, namely, FeF_2, CoF_2, and NiF_2. A very brief report of this work was presented at the Twenty-fourth Annual Conference on Magnetism and Magnetic Materials.[5]

A. Spin structure

The magnetic unit cells of the three compounds FeF_2, CoF_2, and NiF_2 (Fig. 2) have the same dimensions as their chemical unit cells. Each has the rutile crystal structure with cations on a body-centered tetragonal lattice. Below Néel temperature, FeF_2 ($T_N = 79$ K) and CoF_2 ($T_N = 37.7$ K) exhibit a simple two-lattice antiferromagnetic ordering (Fig. 2) in which all spins align along the tetragonal c axis.[6] NiF_2 ($T_N = 73$ K) has an antiferromagnetic ordering along the a axis and the spins are slightly (~0.9°) tilted in the ab plane to give a weak ferromagnetic moment along the b axis.[6]

B. Structure factor

With this knowledge of the spin and crystal structure of the transition-metal difluorides, we see that the scattering cross section is still given by Eq. (3) with the more specific form of $|\vec{Q}|_{\vec{K}=\vec{G}}$ as follows:

$$|\vec{Q}|_{\vec{K}=\vec{G}} = \left| \langle \phi_c | \vec{H} | \phi_c \rangle - e^{\pi i (h+k+l)} \langle \phi_b | \vec{H} | \phi_b \rangle \right|, \tag{5}$$

where $|\phi_c\rangle$ and $|\phi_b\rangle$ are the ground-state wave functions of the corner and body-centered ions,

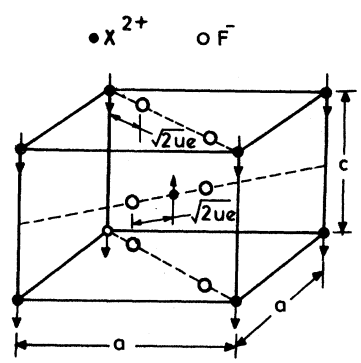

FIG. 2. The accepted unit primitive cell for CoF_2, FeF_2.

respectively.

In each of the compounds the coordination (orthorhombic D_{2h} symmetry) about the corner and body-centered cations differ by a rotation of $\pi/2$ about the c axis. Hence, even though the spin structure is uniaxial, the form factor and the structure factor cannot be easily separated out. We rearrange (see Appendix) the terms to write the structure factor as

$$|\vec{Q}|^2_{\vec{K}=\vec{G}} = |\vec{F}_o|^2 \, |1 - e^{\pi i(h+k+l)}|^2 \quad \text{for } h+k+l \text{ odd}$$

and (6)

$$|\vec{Q}|^2_{\vec{K}=\vec{G}} = |\vec{F}_e|^2 \, |1 + e^{\pi i(h+k+l)}|^2 \quad \text{for } h+k+l \text{ even}.$$

Here $\vec{F}_o$ and $\vec{F}_e$ are effective form factors and are described in terms of the matrix elements of the interaction operator with corner-atom wave functions.

If Eqs. (6) are now plugged in Eqs. (3) and (5) and the resulting equation is compared with the semiclassical spin-only expression of Van Laar,[7] the magnetic form factor will be given by

$$\vec{f}^{\,o}(\vec{K}) = \frac{\vec{F}_o}{|\langle \phi_c | \vec{H} | \phi_c \rangle|_{\vec{K}=0}}, \tag{7}$$

$$\vec{f}^{\,e}(\vec{K}) = \frac{\vec{F}_e}{|\langle \phi_c | \vec{H} | \phi_c \rangle|_{\vec{K}=0}}. \tag{8}$$

As may be seen from the Appendix,

$$\begin{aligned} \vec{F}_o &= \hat{x} f^o_x + \hat{y} f^o_y + \hat{z} f^o_z, \\ \vec{F}_e &= \hat{x} f^e_x + \hat{y} f^e_y + \hat{z} f^e_z, \\ f^o_x &= \frac{\phi_x + \phi'_y}{2}, \quad f^o_y = \frac{\phi_y - \phi'_x}{2}, \quad f^o_z = \phi^+_z, \\ f^e_x &= \frac{\phi_x - \phi'_y}{2}, \quad f^e_y = \frac{\phi_y + \phi'_x}{2}, \quad f^e_z = \phi^-_z. \end{aligned} \tag{9}$$

The symbols o and e tell whether the given form factor exists for odd or even values of $h+k+l$. ϕ_x, ϕ_y, ϕ_z are the matrix elements of the Cartesian components of the magnetic interaction operator in the corner-state wave functions. $\phi'_x, \phi'_y, \phi'_z$ are the matrix elements of the body-centered wave functions but are defined suitably in terms of the corner wave functions (see Appendix). $\vec{f}^{\,o}(\vec{K})$ is a more important quantity than $\vec{f}^{\,e}(\vec{K})$ as it contains the spherical form factor within its f^o_z term. ($f^o_z = f^{os}_z + f^{on}_z$, where the superscripts s and n stand for spherical and nonspherical components.)

IV. POLARIZATION DEPENDENCE OF SCATTERING

For a polarized incident neutron beam, represented by the polarization vector $\vec{P}$, the scattering cross section contains an interference term apart from the magnetic scattering [Eq. (1)] and the nuclear term. This can be evaluated by using Eqs. (10.31) and (10.37) of Marshall and Lovesey[8] with the modification that the operator $\vec{\alpha}$ there is replaced by the operator $\vec{H}$ of Eq. (2) of this paper. The interference term is then given by

$$\left(\frac{d\sigma}{d\Omega}\right)_{\text{int}} = \left(\frac{2\gamma e^2}{m_e c^2}\right) \text{Re}[F_N(\vec{K}) \vec{F}^*_M(\vec{K}) \cdot \vec{P}_\perp], \tag{10}$$

where

$$F_N(\vec{K}) = \sum_n e^{i\vec{K}\cdot\vec{r}_n} \bar{b}_n,$$

$$F^*_M(\vec{K}) = \sum_n e^{-i\vec{K}\cdot\vec{r}_n} \langle q_n | \vec{H} | q_n \rangle,$$

and

$$\vec{P}_\perp = \hat{K} \times \vec{P} \times \hat{K}.$$

For a ferromagnetic substance with identical nuclear and magnetic scattering sites, experiments with neutron spin flipping can be performed as in the spin-only case. The magnetization of the ferromagnet is aligned perpendicular to the scattering plane by an external magnetic field. The Bragg intensities are then measured first with neutron beam polarization parallel and then antiparallel to the magnetization.

Use of Eq. (10) leads to the flipping ratio

$$R = \left[\frac{1 + \left(\frac{\gamma e^2}{m_e c^2}\right) |\langle q | \vec{H} | q \rangle| / \bar{b}}{1 - \left(\frac{e^2}{m_e c^2}\right) |\langle q | \vec{H} | q \rangle| / \bar{b}} \right]^2. \tag{11}$$

In the case of the antiferromagnetic structure in the rutile crystals considered here, the interference term in the cross section is given by

$$\left(\frac{d\sigma}{d\Omega}\right)_{\text{int}} \propto \text{Re}[(2\bar{b}_c + 4\bar{b}_A \cos 2\pi uh \cos 2\pi uk) \times (2\vec{F}_e \cdot \vec{P})] \quad \text{for } h+k+l \text{ even} \tag{12}$$

and

$$\left(\frac{d\Omega}{d\sigma}\right)_{\text{int}} \propto \text{Re}[(-4\bar{b}_A \sin 2\pi uh \sin 2\pi uk) \times (2\vec{F}_o \cdot \vec{P})] \quad \text{for } h+k+l \text{ odd}. \tag{13}$$

Here subscripts c and A refer to cations and an-

ions, respectively, u is the fractional lattice parameter used to locate the anions, and $\vec{F}_o$ and $\vec{F}_e$ are the form factors introduced in Eq. (6).

It is evident from pages 206 and 207 of Ref. 8 that (o,k,l) or (h,o,l) reflections with $k+l$ odd are purely magnetic terms with no polarization effect. All other reflections with $h+k+l$ odd will be mixed nuclear and magnetic, nuclear scattering coming solely from the anions. Since $\vec{F}_o$ is usually very large, the polarization effect, coming from the term $\vec{F}_o \cdot \vec{P}$, is the strongest here. $(h+k+l)$ even reflections are also mixed but the magnetic $(\vec{F}_e)$ and hence the polarization effect is usually very small.

It is important to note that by proper (though laborious) experimental arrangement, $\vec{P}$ can be suitably rotated in the Bragg plane to get a set of values of $\vec{F}_e \cdot \vec{P}$ and $\vec{F}_o \cdot \vec{P}$ by the solving of which unique values of F_e^x, F_e^y, F_e^z, F_o^x, F_o^y, and F_o^z can be obtained. Hence the form factor and the magnetization density distribution could be well defined in the corner and the body-center sites.

V. CALCULATION OF FORM FACTOR

A. Form factor of Co^{2+} in CoF_2

The $3d^7$ ground-state configuration[9] of Co^{2+} gives rise to ^4F as a ground state. Under a cubic field this ground state splits into two orbital triplets $^4\Gamma_4$, $^4\Gamma_5$ and an orbital singlet $^4\Gamma_2$. $^4\Gamma_4$ has the lowest energy. Except for the most detailed discussions, it is customary to neglect the effects of the $^4\Gamma_5$ and $^4\Gamma_2$ manifolds. On the other hand, from symmetry considerations the first excited ^4P state is important. Since the tetragonal field, rhombic field, and spin-orbit coupling are all of the same order of magnitude, computer diagonalization of the Hamiltonian in $^4\Gamma_4$ is the simplest method for a sufficiently accurate determination of the ground state. This is a Kramers doublet. Considering the exchange effect, the explicit form of the ground-state wave function obtained from this is given by[10]

$$\begin{aligned}|\psi_{Co^{2+}}\rangle = &-0.2953\,|0,\tfrac{1}{2}\rangle + 0.3714\,[(\tfrac{3}{8})^{1/2}|-1,\tfrac{1}{2}\rangle + (\tfrac{5}{8})^{1/2}|3,\tfrac{1}{2}\rangle] \\ &+0.7809\,[(\tfrac{3}{8})^{1/2}|1,-\tfrac{3}{2}\rangle + (\tfrac{5}{8})^{1/2}|-3,-\tfrac{3}{2}\rangle] - 0.0556\,|0,\tfrac{3}{2}\rangle \\ &+0.2278\,[(\tfrac{3}{8})^{1/2}|1,\tfrac{1}{2}\rangle + (\tfrac{5}{8})^{1/2}|-3,\tfrac{1}{2}\rangle] + 0.3318\,[|(\tfrac{3}{8})^{1/2}|-1,-\tfrac{3}{2}\rangle + (\tfrac{5}{8})^{1/2}|3,-\tfrac{3}{2}\rangle]\,. \end{aligned} \tag{14}$$

The wave functions $|M_L, M_S\rangle$ are expanded in terms of four hole functions[11] and the matrix elements $\phi_i = \langle\psi_{Co^{2+}}|H_i|\psi_{Co^{2+}}\rangle$ are calculated with the help of the computer program, where $i=x,y,z$. From the expression of ϕ_i in terms of $Y_l^{m'}$s, ϕ_i^+ and ϕ_i^- are separated out by observing their response to the t transformations as mentioned in the Appendix. Table I shows the values obtained therefrom of f_x^o, f_y^o, f_z^{on}, f_z^{os}, f_x^e, f_y^e, and f_z^e for a large number of Bragg peaks; all terms except f_z^{os} are nonspherical.

The spherical magnetic form factor f_z^{os} may be utilized for comparing the theoretical and experimental data. The theoretical expression for this is [from Eq. (7) and the Appendix]

$$\begin{aligned} f_z^{os}(\vec{K}) = (&-1.02369\,\langle J_0\rangle - 0.04318\,\langle J_2\rangle - 0.13120\,\langle J_4\rangle \\ &-0.30999\,\langle g_0\rangle + 0.06634\,\langle g_2\rangle + 0.06649\,\langle g_4\rangle)/(-1.33368)\,. \end{aligned} \tag{15}$$

Here the Freeman-Watson integrals $\langle J_L\rangle = \int_0^\infty R^2(r) j_L(Kr) r^2 dr$, where $j_L(Kr)$ is the spherical Bessel function. The other integrals are

$$\langle g_L\rangle = \int_0^\infty R^2(r) g_L(Kr) r^2 dr\,,$$

where

$$g_L(Kr) = \tfrac{1}{2} i^{-L} \int_{-1}^{+1} f(Kr\mu) P_L(\mu)\, d\mu$$

and $P_L(\mu)$ are the Legendre polynomials. Using the Lovesey relation[12] between $\langle J_L\rangle$ and $\langle g_L\rangle$,

$$f_z^{os}(\vec{K}) = \langle J_0\rangle + 0.29800\,\langle J_2\rangle + 0.13160\,\langle J_4\rangle\,. \tag{16}$$

Watson-Freeman[4] values of $\langle J_L\rangle$ for Co^{2+} may now be used to plot f_z^{os} against $(\sin\theta)/\lambda$ (Fig. 3). The free-ion form factor is also plotted for comparison. The theoretical form factor curve shows an expansion of 10% with respect to the free-ion curve. The total form factor f and the spherical form factor $f_s (= f_z^{os})$ are related as

$$f_s = -f_z^{on} \pm (f^2 - f_x^{o2} - f_y^{o2})^{1/2}\,,$$

as may be simply deduced from

$$\vec{F}_o = x f_x^o + y f_y^o + z f_z^o$$

[Eq. (9)]. A study of Table I reveals the fact that all the nonspherical components of the form factor are very small and hence can be neglected. Therefore $f_s \simeq f$.

Erickson's[6] experimental data lie below even the free-ion form factor curve and as such the experimental curve will be definitely more than 10% contracted with respect to our theoretical curve. This contraction may arise either due to the relativistic effect[13] or due to covalence effect.[14] We

TABLE I. Spherical and nonspherical form factors of Co^{2+} in CoF_2.

No.	*hkl*	f_x^o	f_x^e	f_y^o	f_y^e	f_z^{on}	f_z^e	f_z^{os}
1	100	0	0	0	0	0	0	0.9118
2	010	0	0	0	0	0	0	0.9118
3	001	0	0	0	0	0	0	0.8236
4	110	0	0	0	0	0	0	0.8286
5	101	0.0169	−0.0014	−0.0014	−0.0169	−0.0001	0	0.7611
6	011	−0.0014	0.0169	−0.0169	−0.0014	−0.0001	0	0.7611
7	200	0	0	0	0	+0.0017	0	0.7108
8	111	+0.0140	+0.0140	−0.0171	−0.0171	0.0003	−0.0030	0.7058
9	210	0	0	0	0	0.0009	−0.0085	0.6621
10	201	0.0272	−0.0007	−0.0007	−0.0272	−0.0021	0	0.6161
11	021	−0.0007	0.0272	−0.0272	−0.0007	−0.0021	0	0.6161
12	012	−0.0028	0.0234	−0.0234	−0.0028	−0.0001	0	0.4820
13	102	0.0234	−0.0028	−0.0028	−0.0234	−0.0001	0	0.4820
14	120	0	0	0	0	0.0009	−0.0085	0.6621
15	220	0	0	0	0	0.0086	−0.0153	0.5370
16	022	−0.0027	0.0404	−0.0404	−0.0027	−0.0013	0	0.4033
17	202	0.0404	−0.0027	−0.0027	−0.0404	−0.0013	0	0.4033
18	130	0	0	0	0	−0.0029	−0.0102	0.4728
19	310	0	0	0	0	−0.0029	−0.0102	0.4728
20	103	0.0211	−0.0033	−0.0033	−0.0211	−0.000 04	0	0.2646
21	510	0	0	0	0	−0.0170	−0.0090	0.2105
22	105	0.0114	−0.0026	−0.0026	−0.0114	−0.000 01	0	0.0607
23	222	0.0317	0.0317	−0.0425	−0.0425	0.0043	0.0029	0.3196

would be inclined to discard the relativistic effect since for the 3*d* orbitals the ratio of the relativistic to the nonrelativistic mean value of r is only 1.006 and will consequently result in a very small contraction of the form factor.[15] On the other hand, the fact that covalency can give rise to substantial contraction in the form factor is well established by the work on the $(CrF_5)^{3-}$ cluster[14] in K_2NaCrF_6

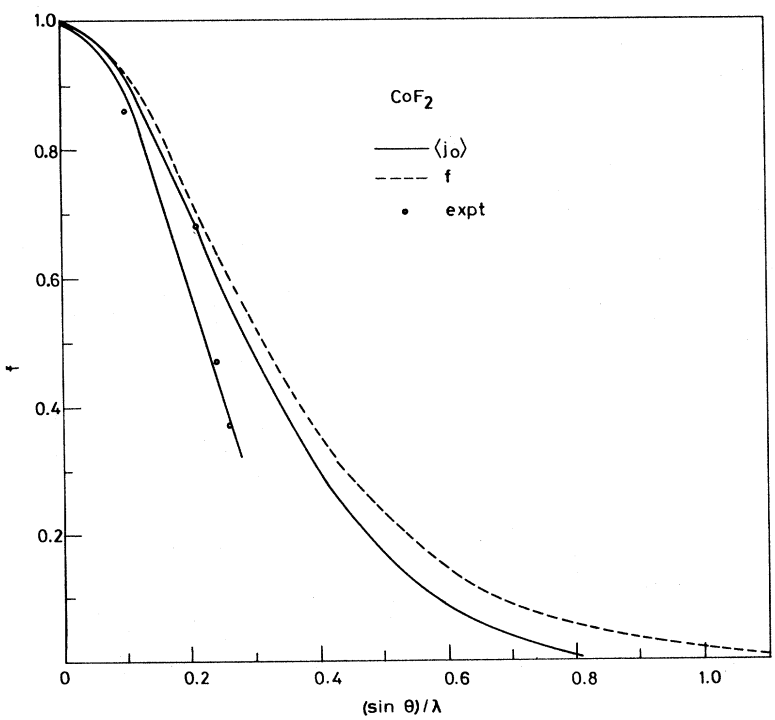

FIG. 3. Form factor of Co^{2+} in CoF_2.

and the $(MnF_6)^{4-}$ cluster[16] in $KMnF_3$. The close proximity (2.02 Å) of Co^{2+} and F^- ions as compared to the nearest-neighbor Co^{2+} ions (3.6796 Å) in CoF_2 strengthens the arguments in favor of covalency effect. The experimental points qualitatively indicate a characteristic forward peaking due to ligands and the low values of f for (201) and (210) peaks suggest an effective reduction of the cationic form factor typical of the covalency effect. Since the data are available only up to $(\sin\theta)/\lambda \sim 0.3$, nothing can be said of the overlap effect.

B. Form factor of Fe^{2+} in FeF_2

In FeF_2 each ferrous ion experience a crystal field originating from six F^- ions that surround it. The Johnston tensor approach has been used by Balcar *et al.*[17] to calculate the scattering cross section and by Balcar[18] to determine the magnetic-moment density distribution of Fe^{2+} in FeF_2. Since the Trammel and the tensor approach are, as demonstrated by Lovesey,[12] basically equivalent, the form factor may also be derived from the tensor expression of Balcar *et al.* for the use of experimentalists.

Referring to Sec. 4.2 of Balcar *et al.*,[17] we note that for their particular choice of $\alpha\vec{K}$ terms, which one has the freedom to add to $\vec{Q}$, $\langle G|\vec{Q}_\perp|G\rangle = \langle G|\vec{Q}|G\rangle$. Hence

$$\langle G|\vec{Q}_\perp|G\rangle = (4\pi)^{1/2}\sum_{KQq} G_q(K,Q)\,Y_Q^K(K)\,,$$

where

$$G_q(K,Q) = \Gamma_q(K'-1,Q)(\langle J_{K'-1}\rangle + \langle J_{K'+1}\rangle)$$

for the orbital case and $G_0(K,Q) = \gamma(K,Q)\langle J_K\rangle$ for the spin case. Nonzero values of $\Gamma_q(K'-1,Q)$ and $\gamma(K,Q)$ are given in their Table I. The transformation for the $G_q(K,Q)$ from the body-center wave function $|G_b\rangle$ to the corner wave function $|G\rangle$ has been worked out by them. This, when utilized, gives the scattering cross section as

$$\frac{d\sigma}{d\Omega} = \left(\frac{\gamma e^2}{mc^2}\right)\sum_q \left|\sum_{K',Q} G_q(K',Q)\,Y_Q^{K'}(K)\left(1+e^{\pi i(h+k+l)}e^{(i\pi/2)(Q-q)}\right)^2\right|. \tag{17}$$

We then expand the $\sum_{q,K',Q}$ in terms of the nonzero $G_q(K',Q)$'s [i.e., $\Gamma_q(K',Q)$ and $\gamma(K',Q)$ of the table]. It may be noted that $\Gamma_q(K',Q)$, with $Q-q$ equal to an odd integer, vanish. For $G_0(K',0)$, $K'=0,2,4$; for $G_0(K',4)$ and $G_0(K',-4)$, $K'=4$, whereas for $G_0(K',2)$ and $G_0(K',-2)$, $K'=2,4$. $G_{-1}(2,1)=G_1(2,1)$ and $G_{-1}(2,1)=G_1(2,1)$. Hence

$$\begin{aligned}\frac{d\Omega}{d\sigma} &= \left(\frac{\gamma e^2}{mc^2}\right)^2\Big[\left|F_e^0(1+e^{\pi i(h+k+l)})+F_o^0(1-e^{\pi i(h+k+l)})\right|^2+\left|F_e^1(1+e^{\pi i(h+k+l)})+F_o^1(1-e^{\pi i(h+k+l)})\right|^2\\ &\qquad+\left|F_e^{-1}(1+e^{\pi i(h+k+l)})+F_o^{-1}(1-e^{\pi i(h+k+l)})\right|^2\Big]\\ &= \left(\frac{\gamma e^2}{mc^2}\right)^2|\vec{F}_o|^2\left|1-e^{\pi i(h+k+l)}\right|^2 \quad \text{for } h+k+l \text{ odd}\\ &= \left(\frac{\gamma e^2}{mc^2}\right)^2|\vec{F}_e|^2\left|1+e^{\pi i(h+k+l)}\right|^2 \quad \text{for } h+k+l \text{ even}.\end{aligned} \tag{18}$$

This is the same as the Trammell formulation equation (6). Here

$$\begin{aligned}F_e^0 &= \sum_{K'}\left[G_0(K',0)Y_0^{K'}(K)+G_0(K',4)Y_4^K(K')\right.\\ &\qquad\left.+G_0(K',-4)Y_{-4}^{K'}(K)\right],\\ F_e^1 &= G_1(2,1)Y_1^2(K)\,,\\ F_e^{-1} &= G_{-1}(2,1)Y_1^2(K)\,,\\ F_o^0 &= \sum_{K'}\left[G_0(K',2)Y_2^{K'}(K)+G_0(K',-2)Y_{-2}^{K'}(K)\right],\\ F_o^1 &= G_1(2,-1)Y_{-1}^2(K)\,,\\ F_o^{-1} &= G_{-1}(2,-1)Y_{-1}^2(K)\,.\end{aligned} \tag{19}$$

The ground-state wave function of Fe^{2+} in FeF_2 is given by

$$\begin{aligned}|\psi_{Fe^{2+}}\rangle &= \left(0.815|0\rangle+\frac{0.580}{\sqrt{2}}(|12\rangle+|1-2\rangle)\right)|M_s=2\rangle\\ &\quad+\frac{(4)0.580}{(1.1)(10^3)\sqrt{2}}(|2\rangle-|-2\rangle)|M_s=2\rangle\,.\end{aligned} \tag{20}$$

The form factors $\vec{F}_o$ and $\vec{F}_e$ can be calculated either by the Trammell method similar to the CoF_2 case or by use of the tensor formalism expressions [Eq. (19)] with the Balcar *et al.*, Table I. Table II gives the spherical and nonspherical parts of the form factor in FeF_2. Table III compares the $|\vec{F}_o|$ and $|\vec{F}_e|$ obtained by the two methods. The Johnston data were obtained by hand calculation, whereas the Trammell data were calculated by the computer. The agreement seems to be excellent, vindicating the correctness of our generalized program.

It is interesting to note that here (as in CoF_2

TABLE II. Spherical and nonspherical form factors of Fe^{2+} in FeF_2.

No.	*hkl*	f_x^o	f_x^e	f_y^o	f_y^e	f_z^{on}	f_z^e	f_z^{os}
1	100	0	0	0	0	0.0001	0	0.8920
2	001	0	0	0	0	0.0172	0	0.8000
3	111	0	0	−0.0096	0.0059	0.0160	0.0143	0.6444
4	200	0	0	0	0	0.0015	0	0.6502
5	020	0	0	0	0	0.0006	0	0.6444
6	012	−0.0074	−0.0056	−0.0074	0.0056	0.0402	0	0.4085
7	021	−0.0107	−0.0077	−0.0107	0.0077	0.0206	0	0.5348
8	210	0	0	0	0	−0.0005	0.0218	0.5891
9	003	0	0	0	0	0.0395	0	0.1930
10	013	−0.0063	−0.0057	−0.0063	0.0057	0.0431	0	0.1837
11	103	0.0063	0.0057	0.0063	0.0057	0.0431	0	0.1837
12	130	0	0	0	0	0.0012	0.0183	0.3986
13	202	0.0136	0.0102	−0.0136	0.0102	0.0425	0	0.3226
14	022	−0.0136	−0.0102	−0.0136	0.0102	0.0425	0	0.3226
15	220	0	0	0	0	−0.0031	0.0306	0.4557
16	023	−0.0128	−0.0116	−0.0128	0.0116	0.0503	0	0.1403
17	041	−0.0160	−0.0130	−0.0160	0.0130	0.0223	0	0.1948
18	024	−0.0098	−0.0097	−0.0098	0.0097	0.0417	0	0.0342
19	240	0	0	0	0	−0.0024	0.0207	0.1677
20	025	−0.0067	−0.0083	−0.0067	0.0083	0.0318	0	−0.0039
21	052	−0.0253	−0.0223	−0.0253	0.0223	0.0418	0	0.0558
22	016	−0.0021	−0.0032	−0.0021	0.0032	0.0194	0	−0.0189
23	061	−0.0156	−0.0135	−0.0156	0.0135	0.0196	0	0.0340

also) the "forbidden" peaks with $(h+k+1)$ even arise due to the difference in the ligand coordination about the two cations even when we do not consider the presence of unpaired electron spin on the ligand F^{-1} ions. The effect, as expected, is small, as may be seen from the values of f_x^e, f_y^e, and f_z^e. The important contribution to the aspherical part comes mainly from the f_z^{on} term which may sometimes be as large as 75% of the spherical part (052 peak) and may even be much greater than the spherical term (025).

TABLE III. Comparison of the form factor of FeF_2 by the Trammell and Johnston method.

	f_o		f_e	
Peak	Trammell	Johnston	Trammell	Johnston
100	0.8921	0.8926	0	0
001	0.8172	0.8127	0	0
111	0.6605	0.6544	0.0143	0.0137
200	0.6517	0.6518	0	0
012	0.4489	0.4344	0	0.0050
210	0.5886	0.5900	0.0218	0.0288
021	0.5556	0.5689	0.0100	0.0060
003	0.2325	0.2106	0	0
013	0.2268	0.2071	0	0.0040
103	0.2268	0.2071	0	0.0040
130	0.3998	0.4007	0.0183	0.0169
202	0.3654	0.3475	0.0141	0.0060
022	0.3654	0.3475	0.0141	0.0060
220	0.4526	0.4602	0.0306	0.0295
023	0.1915	0.2043	0.0141	0.0076
041	0.2184	0.2152	0.0141	0.0034
024	0.0775	0.0550	0.0141	0.0058
240	0.1653	0.1665	0.0207	0.0189
025	0.0279	0.0061	0.0141	0.0041
052	0.1034	0.0933	0.0316	0.0079
016	0.0005	0.0219	0	0.0016

The analytical expression for the spherical magnetic form factor is

$$f^s_{Fe^{2+}}(\vec{K}) = \langle J_0\rangle + 0.030\langle J_2\rangle - 0.164\langle J_4\rangle . \qquad (21)$$

Using the values of $\langle J_0\rangle$, $\langle J_2\rangle$, and $\langle J_4\rangle$ as tabulated by Watson and Freeman,[4] $f^s_{Fe^{2+}}$ is plotted against $(\sin\theta)/\lambda$ in Fig. 4. As is evident, there is a uniform contraction of about 3% with respect to the free-ion curve. The available experimental data[6] are meager.

C. Form factor of Ni^{2+} in NiF_2

Divalent nickel[19] has eight $3d$ electrons and the free ion has a ground state $^3F_4$. The sevenfold orbital degeneracy is removed in part by a cubic field, resulting in a low-lying orbital singlet and two higher triplet states. The orbital singlet is threefold degenerate in spin quantum number. This degeneracy is removed by the application of exchange field.

The ground-state wave function, after the application of exchange field, will be[20]

$$\phi_c = \phi_{-1} + \frac{\lambda}{10Dq}(\Gamma_5^{(c)}) , \qquad (22)$$

where

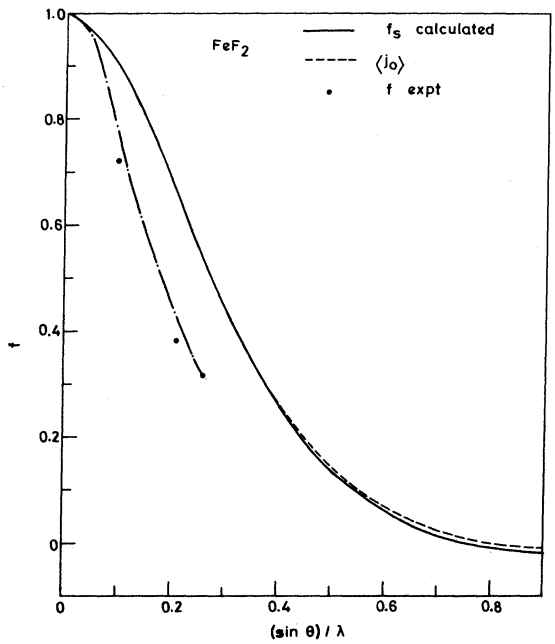

FIG. 4. Form factor of Fe^{2+} in FeF_2.

$$\phi_{-1}=\frac{1}{\sqrt{2}}(Y_3^2-Y_3^{-2})\psi_{-1}$$

and

$$(\Gamma_5^{(c)})=\tfrac{1}{2}(\theta_2\psi_{-1}-i\theta_3\psi_0)\,.$$

Here

$$\theta_2=\frac{1}{\sqrt{2}}(Y_3^2+Y_3^{-2}),\quad \theta_3=(\tfrac{5}{8})^{1/2}Y_3^{-1}-(\tfrac{3}{8})^{1/2}Y_3^3\,,$$

$$\psi_1=\alpha\alpha,\quad \psi_{-1}=\beta\beta,\quad \psi_0=\frac{1}{\sqrt{2}}(\alpha\beta+\beta\alpha)\,.$$

ψ_0, ψ_1, ψ_{-1} are spin states. Y's are spherical harmonics. $10Dq$ is the energy difference between the low-lying orbital singlet and the next triplet.

For form factor calculation the spin structure of NiF_2 may be considered as the superposition of an antiferromagnetic structure with spin along $\pm a$ direction and a very weak (percentage magnetic moment 1.55%) ferromagnetic structure with spin along $+b$ direction.[21] The form factor expression for the ferromagnetic structure is the same as given in the Appendix except for the fact that f^o and f^e components are interchanged. The nonspherical terms are very small and may be neglected. The calculation for the antiferromagnetic structure is more elaborate but may be brought in the same final form as in the Appendix.

The expression for the spherical form factor is

$$f^s_{Ni^{2+}}(\vec{K})=\langle J_0\rangle+0.0327\langle J_2\rangle+0.5379\langle J_4\rangle\,. \qquad (23)$$

Table IV gives the spherical and nonspherical parts of the form factor in NiF_2 for various peaks. It may be noted that aspherical terms are mostly negligible in the present case. Hence the magnetization density has, for all practical purposes, a spherical distribution about the lattice points.

Using the values of $\langle J_0\rangle$, $\langle J_2\rangle$, and $\langle J_4\rangle$ as tabulated by Watson and Freeman,[4] $f^s_{Ni^{2+}}$ in Eq. (23) is plotted against $(\sin\theta)/\lambda$ in Fig. 5. There is a uniform expansion of about 15% with respect to the free-ion curve. Experimental data, again, are too meager to draw any conclusions.

VI. COMPARISON OF FORM FACTORS

It is evident from the preceding section that the complete use of the present analysis can only be made when a sufficient amount of experimental da-

TABLE IV. Spherical and nonspherical form factors of Ni^{2+} in NiF_2.

No.	*hkl*	f^e_x	f^o_x	f^e_y	f^o_y	f^e_z	f^o_z	f_{zs}
1	100	0	0	0	0	0	0	0.9157
2	001	0	0	0	0	0	0	0.8057
3	110	0	0	0	0	0	0	0.8273
4	101	0.000 06	0.0005	−0.0005	0.000 28	−0.000 35	0	0.7509
5	200	0	0	0	0	−0.0045	0	0.6992
6	111	0	−0.000 02	0.000 52	0.0005	0.001	0	0.6843
7	210	0	0	0	0	0.0012	0	0.6399
8	201	0.000 01	0.000 01	0.0005	0.0005	−0.0021	0	0.5902
9	012	−0.0003	0.0003	−0.0009	0.0003	0.0001	0	0.4520
10	220	0	0	0	0	0.009	0	0.5260
11	022	0.0004	−0.0017	0.0014	0.0006	−0.0011	0	0.3751
12	310	0	0	0	0	−0.0018	0	0.5584
13	320	0	0	0	0	0.0111	0	0.3849
14	302	0.0002	0.002	−0.001	0.0011	−0.0063	0	0.2835
15	340	0	0	0	0	0.0228	0	0.2386
16	720	0	0	0	0	−0.0169	0	0.0754
17	920	0	0	0	0	−0.0245	0	0.0494

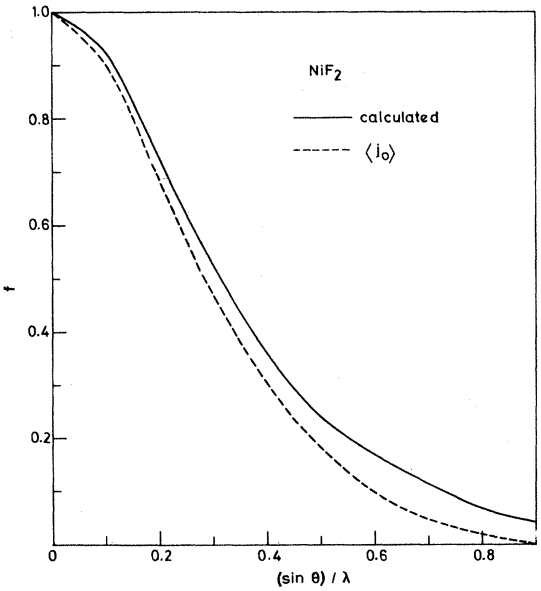

FIG. 5. Form factor of Ni^{2+} in NiF_2.

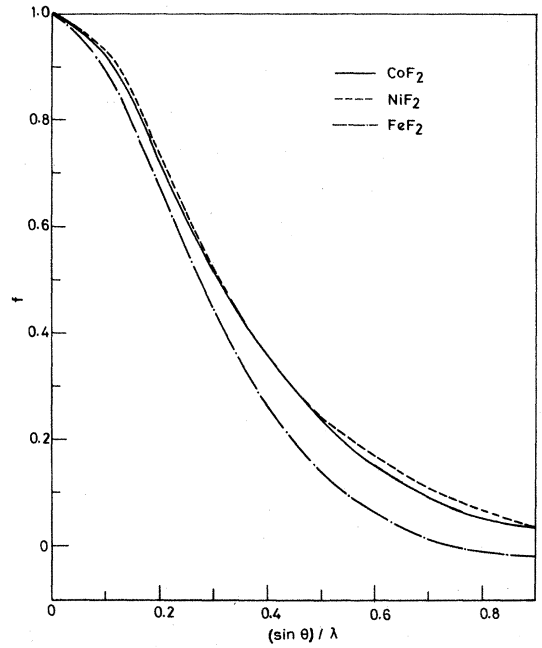

FIG. 6. Comparison of the form factors of transition-metal ions in their difluorides.

ta is available. The deviation of the present data from the experimental ones is a measure of the covalency effect and this deviation may be utilized to determine the covalency parameters. Once this is known, the exchange constant and other magnetic quantities can be evaluated.

However, interesting observations on weakly covalent systems may be made with the framework of crystal-field theory as an approximation by a comparative study of the form factor graphs. To begin with, a look into the Freeman-Watson data[4] for the free-ion form factors shows that the following are true: (i) In all three cases of Fe, Co, and Ni the form factor expands with ionization. This is due to the fact that the effective radius of the ion decreases with ionization. (ii) Ions with different nuclear charge (Z values) and the same number of d electrons show an expansion of the form factor with increase in Z value. This is a reflection of the fact that the electronic charge tends to concentrate closer to the nucleus with the increase of the nuclear charge. The free-ion spin-only form factors of Fe^{2+}, Co^{2+}, and Ni^{2+} ions expand with increasing Z as in case (ii). However, it has to be remembered that the number of d electrons increases from Fe^{2+} to Ni^{2+}, i.e., the effective radius increases, whose effect is to contract the form factor. That there is an overall expansion shows that the effect of nuclear attraction on the electronic charge distribution with unpaired spin is very dominant.

Figure 6 shows the form factors of Fe^{2+}, Co^{2+}, and Ni^{2+} in their difluorides. It is evident that the trend of the form factor expanding with increasing Z is maintained even when the orbital effect is included. The form factors of Fe^{2+}, Co^{2+}, and Ni^{2+} in several other compounds have been determined by Khan and collaborators.[11,22] Figure 7 shows the result of calculation for these ions in KXF_3 ($X = Fe^{2+}$, Co^{2+}, Ni^{2+}). Whereas the expansion sequence is maintained for Fe^{2+} and Co^{2+}, it is inver-

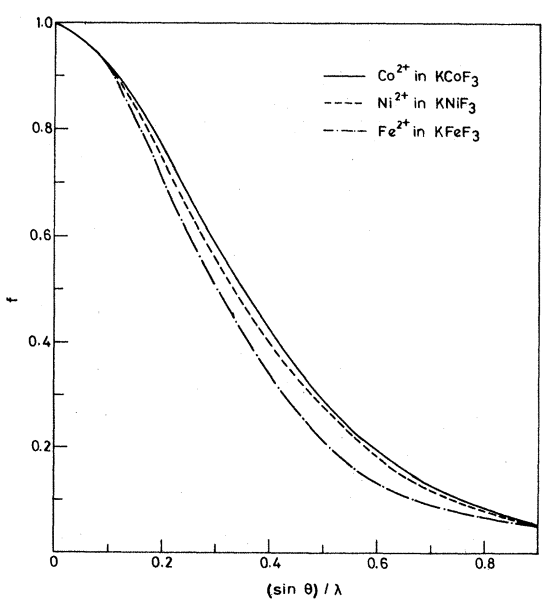

FIG. 7. Comparison of the form factors of transition-metal ions in their potassium trifluorides.

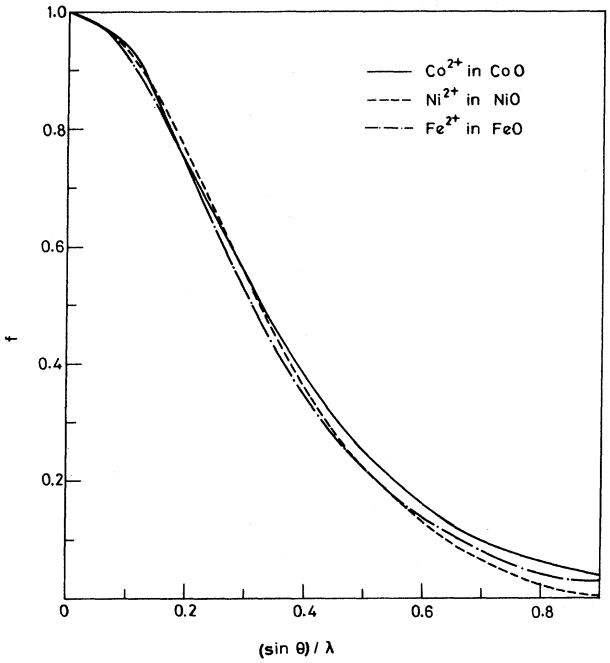

FIG. 8. Comparison of the form factors of transition-metal ions in their oxides.

ted in the case of Co^{2+} and Ni^{2+}. Figure 8 shows the results for XO compounds, where $X = Fe^{2+}$, Co^{2+}, Ni^{2+}. The result is halfway between the last two cases. The Fe^{2+}–Co^{2+} sequence is maintained. Ni^{2+} is expanded with respect to Co^{2+} up to $(\sin\theta)/\lambda \sim 0.3$, but crosses and gets below the Co^{2+} curve beyond this, and finally for $(\sin\theta)/\lambda \sim 0.58$ even falls below the Fe^{2+} curve. The general trend of expansion of the form factor with increasing Z is partly due to the fact that the unquenched orbital momentum is small compared to the spin and as such does not affect the trends of the spin curve in a substantial manner. However, a perusal of Table V columnwise shows that the role of the orbital moment should not be underestimated. In fact, except in the case of FeF_2, the orbital moment *distribution* is more strongly contracted than the spin distribution. Also, in the case of difluorides, the expansion sequence of the form factor with respect to "spin only" with increasing Z is maintained. In the case of the potassium trifluorides and oxides also the sequence is maintained for Fe^{2+}–Co^{2+}. However, it would be naive to link it with the nuclear Coulomb effect rather than to the number of interacting electrons. Since the interactions involved are complicated and many (Coulomb repulsion, spin-orbit, crystal field, and exchange), it is difficult to link the fact of orbital moment density distribution to a single parameter. The anomalous behavior of the Ni^{2+} form factor in the potassium trifluorides and oxides is evidently connected to the fact that the ground state is singlet and the orbital moment comes only from the excited states.

TABLE V. Expansion or contraction of theoretical curves with respect to free-ion curves.

	FeF_2	$KFeF_3$	FeO
Fe^{2+}	3% contraction	10% expansion	9% expansion
	CoF_2	$KCoF_3$	CoO
Co^{2+}	10% expansion	15% expansion	11% expansion
	NiF_2	$KNiF_3$	NiO
Ni^{2+}	15% expansion	6% expansion	4% expansion

The effect of the crystal fields is clearly brought out by plotting the form factors of the same ion (say, Co^{2+}) in different substances. It is seen that the crystal field also plays a dominant role in expanding or contracting the magnetization density distribution. The fluorides of the metals (Fe^{2+}, Co^{2+}, Ni^{2+}) have the rutile, the potassium trifluorides have the perovskite, and the oxides have the face-centered cubic structure. Figure 9 shows the form factor of Fe^{2+} in the above three crystalline environments. It is found that in the rutile structure there is a 3% contraction, whereas in the other two there are substantial expansions. Figure 10 shows the case of Co^{2+} in the crystalline environments of the above three kinds. It is seen that in all the cases there are substantial expansions of the form factor. Finally, Fig. 11 depicts the form factors of Ni^{2+} in these en-

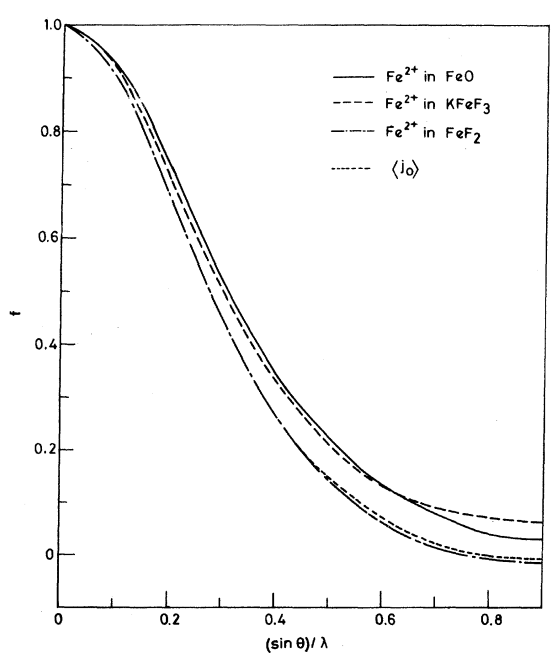

FIG. 9. Form factors of Fe^{2+} in different crystalline environments.

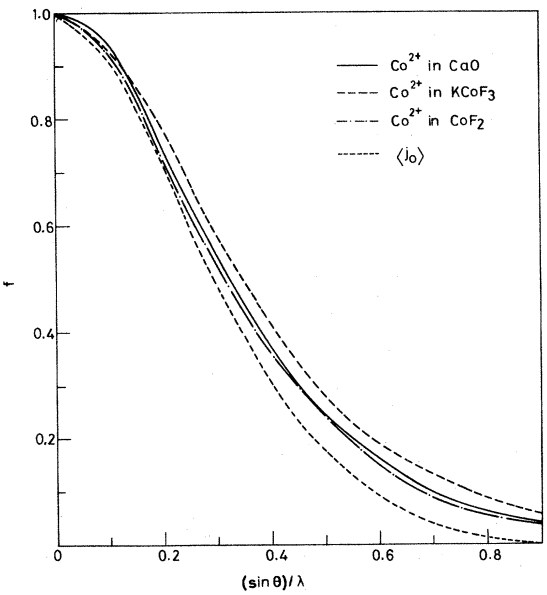

FIG. 10. Form factors of Co^{2+} in different crystalline environments.

vironments. Here also the general trend is expansion. The conclusion that may be drawn is that, in general, the crystalline environments tend to contract the magnetization density distribution of the magnetic electron systems. The case of Ni^{2+} is to be specially noticed; the magnetization density distribution pattern is distinctly different from the iron and cobalt ion case. It may be recalled that out of the three ions studied,

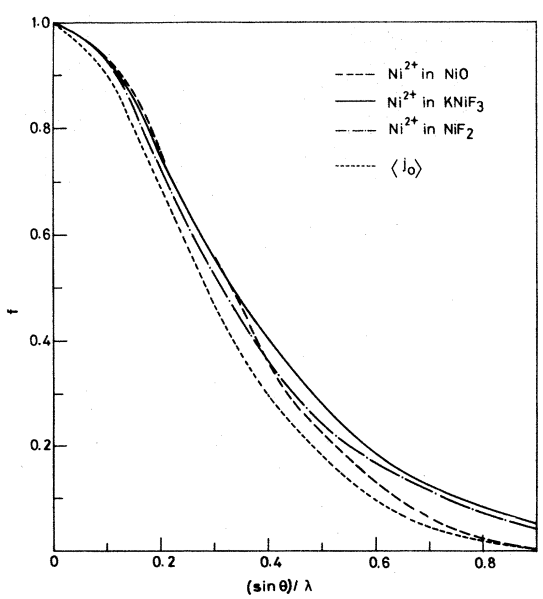

FIG. 11. Form factors of Ni^{2+} in different crystalline environments.

only Ni^{2+} has the singlet ground state in the cubic crystalline field. Table V shows the complete list of the orbital effect (expansion or contraction with respect to the free-ion value) of the compounds discussed herein. They give us a comparative estimate of the partially quenched orbital moment distributions in these substances, that is, the effect of the excited states of the free ion on the ground state through spin-orbit coupling.

Finally, the question of quenching is quantitatively studied by writing the form factor expression as

$$f=\frac{\mu_s}{\mu}f^{\text{spin}}+\frac{\mu_0}{\mu}f^{\text{orbit}} .$$

Obviously, the coefficient of f^{orbit} is the fractional orbital magnetic moment of the ion. Table VI gives the theoretically calculated μ_0/μ for the compounds discussed in this section. We may note that this quantity is the same as $(g-2)/g$, where g is the g factor of the ion in the solid. g may be experimentally determined by resonance, and so provides a means of comparing our theoretical data with the experimental ones. However, resonance data are usually given in terms of the g factor (spectroscopic splitting factor) which is the coefficient of an effective spin s. This g may be related to but different from our g. Correct experimental data were available only for FeF_2 (Ref. 23) where the agreement between the theoretical and experimental data is seen to be very good. Experimental data are in the form of $(g-2)/g$. They are put in the parentheses below μ_0/μ values. In the case of NiF_2 the experimental data correspond to Ni^{2+} in ZnF_2 (Ref. 24), where CoO result corresponds to Co^{2+} in MgO (Ref. 25) and FeO to Fe^{2+} in MgO (Ref. 26). In these cases the agreements are not, as could be expected, so satisfactory but are good enough to give confidence on the general correctness of the calculations.

VII. CONCLUSION

In this work the authors have reformulated the Trammell neutron scattering cross section in a

TABLE VI. Theoretical and experimental quenching parameters μ_0/μ.

CoF_2	$KCoF_3$	CoO
0.23	0.30	0.30
FeF_2	$KFeF_3$	(0.53)
0.09	0.19	FeO
(0.11)	(0.07)	0.25
NiF_2	$KNiF_3$	(0.41)
0.04	0.14	
(0.14)		

form easily amenable to computer calculation and have written an elaborate computer program for calculation of the form factor for any given wave function. Though it does not have the theoretical elegance of the Johnston tensor approach and is not as general as the Stassis and Deckman[27] formulation, it is as effective as either of them for the transition-metal compounds and for many of the rare-earth compounds. The real impact of the present work lies in the fact that it opens up the possibility of simultaneously working out the form factors of a large number of compounds and of having a comparative study of them. A listing of computer programs 1 and 2 will be available on request from any one of the authors.

ACKNOWLEDGMENTS

The authors are indebted to Mr. N. Roberts for his help in the writing of the computer program and Mr. Ram Narayan for his collaboration in the derivation of the ground-state wave function of Ni^{2+} in NiF_2.

APPENDIX

The structure factor in the Trammell form is given by

$$(\vec{Q})_{\vec{K}=\vec{G}} = |\langle\phi|\vec{H}|\phi\rangle - e^{\pi i(h+k+l)}\langle\phi_c|\vec{H}|\phi_c\rangle| ,$$

where $|\phi\rangle$ and $|\phi_c\rangle$ represent the ground-state wave functions of the corner and the body-centered ions, respectively. The negative sign comes from the fact that the spin is inverted between the two sites. Now $|\phi_c\rangle = R|\phi\rangle$ in CoF_2, where R is the operator for rotation by $-\pi/2$ about the z axis or the crystal c axis. Thus,

$$(\vec{Q})_{\vec{K}=\vec{G}} = |\langle\phi|\vec{H}|\phi\rangle + e^{\pi i(h+k+l)}\langle\phi|R^{-1}\vec{H}R|\phi\rangle|$$
$$= |\hat{x}\langle\phi|H_x|\phi\rangle + \hat{y}\langle\phi|H_y|\phi\rangle + \hat{z}\langle\phi|H_z|\phi\rangle - (\hat{x}\langle\phi|H_y|\phi\rangle^t - \hat{y}\langle\phi|H_x|\phi\rangle^t + \hat{z}\langle\phi|H_z|\phi\rangle^t)e^{\pi i(h+k+l)}| ,$$

where superscript t means that the effect of this rotation on $Y_1^m(K)$'s is yet to be performed. Writing the matrix elements in a compact form,

$$(\vec{Q})_{\vec{K}=\vec{G}} = |\hat{x}\phi_x + \hat{y}\phi_y + \hat{z}\phi_z + (\hat{x}\phi_y^t - \hat{y}\phi_x^t + \hat{z}\phi_z^t)e^{\pi i(h+k+l)}| .$$

Now, ϕ_x, ϕ_y, and ϕ_z can each be split into two parts, $\phi_i = \phi_i^+ + \phi_i^-$, depending on their response to the t transformations on $Y_1^m(K)$'s.

$$(\vec{Q})_{\vec{K}=\vec{G}} = |\hat{x}(\phi_x^+ + \phi_x^-) + \hat{y}(\phi_y^+ + \phi_y^-) + \hat{z}(\phi_z^+ + \phi_z^-) + \hat{x}i(\phi_y^+ - \phi_y^-) - \hat{y}i(\phi_x^+ - \phi_x^-) + \hat{z}(\phi_z^+ - \phi_z^-)e^{\pi i(h+k+l)}| .$$

Writing $i(\phi_x^+ - \phi_x^-) = \phi_x'$ and $i(\phi_y^+ - \phi_y^-) = \phi_y'$ (ϕ_x', ϕ_y' being real),

$$(\vec{Q})_{\vec{K}=\vec{G}} = |\hat{x}(\phi_x - \phi_y' e^{\pi i(h+k+l)}) + \hat{y}(\phi_y + \phi_x' e^{\pi i(h+k+l)})$$
$$+ \hat{z}[\phi_z^+(1 - e^{\pi i(h+k+l)}) + \phi_z^-(1 + e^{\pi i(h+k+l)})]| .$$

By adding and subtracting the same terms,

$$(\vec{Q})_{\vec{K}=\vec{G}} = |\tfrac{1}{2}[\hat{x}(\phi_x + \phi_y') + \hat{y}(\phi_y - \phi_x') + \hat{z}\phi_z^+(1 - e^{\pi i(h+k+l)})]$$
$$+ \tfrac{1}{2}[\hat{x}(\phi_x - \phi_y') + \hat{y}(\phi_y + \phi_x') + \hat{z}\phi_z^-(1 + e^{\pi i(h+k+l)})]| .$$

Setting $f_x^o = \frac{1}{2}(\phi_x + \phi_y')$, $f_x^e = \frac{1}{2}(\phi_x - \phi_y')$, etc.,

$$(\vec{Q})_{\vec{K}=\vec{G}} = |(\hat{x}f_x^o + yf_y^o + \hat{z}f_z^o)(1 - e^{\pi i(h+k+l)}) + (\hat{x}f_x^e + \hat{y}f_y^e + \hat{z}f_z^e)(1 + e^{\pi i(h+k+l)})|$$
$$= |\vec{F}_o(1 - e^{\pi i(h+k+l)}) + \vec{F}_e(1 + e^{\pi i(h+k+l)})| .$$

[1]G. T. Trammell, Phys. Rev. 92, 1387 (1953).

[2]M. Blume, Phys. Rev. 124, 96 (1961).

[3]E. U. Condon and G. H. Shortley, *The Theory of Atomic Spectra* (Cambridge University Press, New York, 1935).

[4]R. E. Watson and A. J. Freeman, Acta Crystallogr. 14, 27 (1961).

[5]D. C. Khan and S. M. Kirtane, J. Appl. Phys. 50, 1963 (1979).

[6]R. A. Erickson, Phys. Rev. 90, 779 (1953); A. H. Cooke, K. A. Gehring, and R. Lazenby, Proc. R. Soc. London 85, 967 (1965).

[7]B. Van Laar, Ph.D. thesis, University of Leiden, 1968 (unpublished).

[8]W. Marshall and S. W. Lovesey, *Theory of Thermal Neutron Scattering* (Clarendon, Oxford, 1971), pp.

329 and 330.
[9]P. Martel, R. A. Cowley, and R. W. H. Stevenson, Can. J. Phys. 46, 1355 (1968).
[10]H. M. Gladney, Phys. Rev. 146, 253 (1966).
[11]A. Mahendra and D. C. Khan, Phys. Rev. B 4, 3901 (1971).
[12]S. W. Lovesey, J. Phys. C 2, 470 (1969).
[13]A. J. Freeman, J. P. Desclaux, G. H. Lander, and J. Faber, Jr., Phys. Rev. B 13, 1168 (1976).
[14]F. A. Wedgewood, Proc. R. Soc. London A349, 447 (1976).
[15]J. P. Desclaux, private communication.
[16]A. J. Freeman and D. E. Ellis, Phys. Rev. Lett. 24, 516 (1970).
[17]E. Balcar, S. W. Lovesey, and F. A. Wedgwood, J. Phys. C 6, 3746 (1973).
[18]E. Balcar, J. Phys. C 8, 1581 (1975).
[19]W. Low, Phys. Rev. 109, 247 (1958).
[20]S. M. Kirtane, Ph.D. thesis, Indian Institute of Technology, Kanpur, 1978 (unpublished).
[21]R. A. Alikhanov, Zh. Eksp. Teor. Fiz. 37, 1145 (1959) [Sov. Phys.—JETP 10, 814 (1960)].
[22]J. K. Sharma and D. C. Khan, Phys. Rev. B 14, 4184 (1976).
[23]R. C. Ohlman and M. Tinkham, Phys. Rev. 123, 425 (1961).
[24]M. Peter and J. B. Mock, Phys. Rev. 118, 137 (1960).
[25]D. J. I. Fry and P. M. Llewellyn, Proc. R. Soc. London A266, 84 (1962).
[26]B. H. McMahon, Phys. Rev. 134, A128 (1964).
[27]C. Stassis and H. W. Deckman, Phys. Rev. B 12, 1885 (1975).